

Synthesis of Extended Graphdiyne Wires by Vicinal Surface Templating

Borja Cirera,[†] Yi-Qi Zhang,[†] Jonas Björk,[§] Svetlana Klyatskaya,[‡] Zhi Chen,[‡] Mario Ruben,^{||,‡} Johannes V. Barth,[†] and Florian Klappenberger*,[†]

[†]Physik Department E20, Technische Universität München, James-Franck-Straße, 85748 Garching, Germany

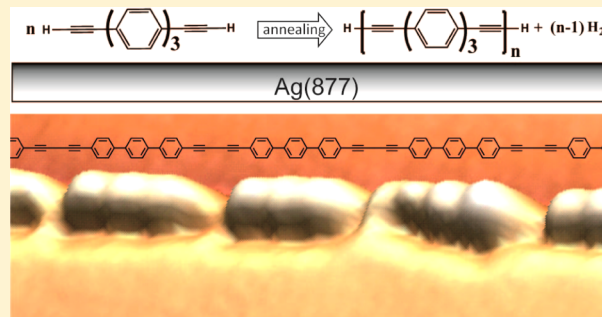
[‡]Institute of Nanotechnology, Karlsruhe Institute of Technology, 76344 Eggenstein-Leopoldshafen, Germany

[§]Department of Physics, Chemistry, and Biology (IFM), Linköping University, 58183 Linköping, Sweden

^{||}IPCMS-CNRS University de Strasbourg, 23 Rue de Loess, 67034 Strasbourg France

Supporting Information

ABSTRACT: Surface-assisted covalent synthesis currently evolves into an important approach for the fabrication of functional nanostructures at interfaces. Here, we employ scanning tunneling microscopy to investigate the homocoupling reaction of linear, terminal alkyne-functionalized polyphenylene building-blocks on noble metal surfaces under ultrahigh vacuum. On the flat Ag(111) surface, thermal activation triggers a variety of side-reactions resulting in irregularly branched polymeric networks. Upon alignment along the step-edges of the Ag(877) vicinal surface drastically improves the chemoselectivity of the linking process permitting the controlled synthesis of extended-graphdiyne wires with lengths reaching 30 nm. The ideal hydrocarbon scaffold is characterized by density functional theory as a 1D, direct band gap semiconductor material with both HOMO and LUMO-derived bands promisingly isolated within the electronic structure. The templating approach should be applicable to related organic precursors and different reaction schemes thus bears general promise for the engineering of novel low-dimensional carbon-based materials.



KEYWORDS: Covalent coupling, terminal alkyne, stepped surface, chemoselectivity, graphdiyne

The extremely versatile bonding capabilities of carbon result in a practically unlimited pool of carbon allotropes and carbon-rich scaffolds.^{1–3} The enormous success of fullerenes, carbon nanotubes, and graphene has inspired scientists to speak of the era of carbon allotropes.⁴ Within this movement, the interest in low-dimensional hydrocarbon materials derived from carbyne, graphyne, or graphdiyne was strongly revitalized.^{5–7} In solution chemistry, acetylenic scaffolding provides a most important approach to the synthesis of such compounds. The synthetic pathways mainly rely on acetylenic coupling reactions,^{2,8,9} whereby templates have been successfully used to achieve specific geometries.^{10–12} With these methods also molecular wires such as poly(phenyleneethynylene)s^{13–15} or poly(phenylenebutadiynylene)s¹⁶ can be synthesized that present significant promise for molecular electronics^{17,18} and organic photovoltaic devices.^{16,17} However, the production of high-quality one-dimensional (1D) polymers is strongly hampered by unwanted side-reactions such as spurious cross-linking leading to 2D organic materials even when starting with linear ditopic monomers.¹⁹ Multistep strategies can be employed to prepare well-defined long-chain oligomers in solution,^{14,15,20,21} however solubility-providing side-chains have to be attached to the

repeat units for product purification and separation.^{13,20} Thus, there is a strong demand for novel and simpler production approaches toward well-defined, unsubstituted π -conjugated molecular wires.

Over the last years, surface-assisted covalent synthesis has been established as an alternative route toward the fabrication of novel materials. Graphene of technologically relevant quality was grown on Cu foil and then transferred to the desired substrate.²² Furthermore, a multitude of covalent molecular nanoarchitectures has been realized in a bottom-up fashion from carefully designed building-blocks with various methods such as the Ullmann coupling,^{23–27} polyamide formation,^{28–30} Cu adatom mediated C–C coupling,^{31,32} and condensation reactions.^{33–35}

Recently, we introduced C–C scaffolding under on-surface conditions by covalent homocoupling of terminal alkynes on a noble metal.³⁶ Thereby it was observed that on Ag(111), the C–C coupling takes place via a concerted multistep reaction mechanism, proceeding via initial formation of a covalently

Received: December 17, 2013

Revised: February 10, 2014

Published: February 24, 2014

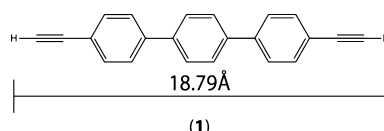


linked dimer and subsequent dehydrogenation and butadiyne bridge formation.^{36,37} This approach allows for the controlled synthesis of novel molecular species by dimerization but exhibits poor chemo- and regioselectivity when targeting extended low-dimensional architectures resulting in a mixture of products.^{38–41} Here, we specifically target one-dimensional (1D) carbon-rich materials, whence strictly linear reaction products are mandatory. This condition excludes on the one hand the use of the related azide–alkyne cycloaddition^{42,43} yielding linkages with angles between adjacent monomers intrinsically deviating from the desired 180°. On the other hand, when working with alkyne homocoupling reactions on planar substrates there is a clear tendency toward the formation of branched oligomers and irregular, reticulated 2D networks^{36,38–41} that represents a major obstacle. Thus, for the controlled fabrication of a regular 1D polymer we employ a rodlike ditopic compound and explore a surface templating effect,⁴⁴ suppressing the unwanted branching side reactions of the alkyne homocoupling. We notably demonstrate that vicinal surfaces, presenting a regular step-terrace topology, can guide reactions with an inherent complex pathway and missing chemoselectivity. By exploiting favored alignment at the step edges of a vicinal surface, we obtain preferential regiospecific C–C linking, providing the desired linear oligomeric arrangement. Applying this vicinal surface templating allows producing a novel 1D hydrocarbon scaffold, namely the poly(terphenylene-butadiynylene) $[-C\equiv C-Ph_3-C\equiv C-]_n$ that can be regarded as an extended-graphdiyne molecular wire. The generated organic polymer is the first representative of the family of poly(oligophenylene-butadiynylene)s, distinct from the more common poly(phenylene-butadiynylene)s^{16,19,45,46} by the presence of several adjacent phenylene moieties in each monomer. The latter feature is important for tuning the energy gap⁴⁷ and the band structure^{48,49} of the resulting π -conjugated polymer that represents a prospective 1D organic semiconductor.^{16,17}

The experiments were carried out in a home-built Besocke-type scanning tunneling microscope (STM) at liquid nitrogen temperature (~ 90 K) in UHV ($\sim 10^{-10}$ mbar) conditions. The samples were prepared *in situ* under UHV, by evaporating the molecules by means of organic molecular beam epitaxy (OMBE) on precleaned silver surfaces. The theoretical part of the study was performed by periodic density functional theory (DFT) calculations using the VASP code⁵⁰ with the projected augmented wave method⁵¹ and the PBE exchange-correlation functional.⁵² The plane waves were expanded to a cutoff of 500 eV. Further details are described in the Supporting Information.

The employed compound 4,4"-diethynyl-1,1':4',1"terphenyl (**1**) is depicted in Scheme 1 (detailed information about the synthesis can be found in the Supporting Information). The molecule exhibits C_{2v} symmetry featuring a distance between the terminal hydrogens of 18.79 Å, as obtained from DFT

Scheme 1. Chemical Structure of 4,4"-Diethynyl-1,1':4',1"terphenyl (1)^a



^aLength refers to the distance between terminal hydrogen atoms.

calculations. The three arene rings between the terminal alkynes act as a rigid backbone, whose combined configuration shows, in analogy with the respective dicarbonitrile polyphenyl species, a small twisting angle between adjacent phenyl rings.⁵³ Moreover, due to the increased σ -character and hence electronegativity of the ethynyl carbons, the terminal H atoms show an increased acidity compared to carbon atoms with single and double bonds.⁵⁴ This feature entails high reactivity and notably permits the previously observed surface-assisted homocoupling.³⁶

With the aim of producing linear molecular wires through surface-assisted acetylenic homocoupling mechanism (Figure 1a), **1** was initially deposited onto the Ag(111) surface held at 250 K, followed by an annealing step at 400 K to trigger covalent bond formation. The result is depicted by the STM data in Figure 1b, evidencing regiospecific pathways where exclusively the terminal ethyne groups are interconnected. Although linear homocoupled oligomeric compounds (green

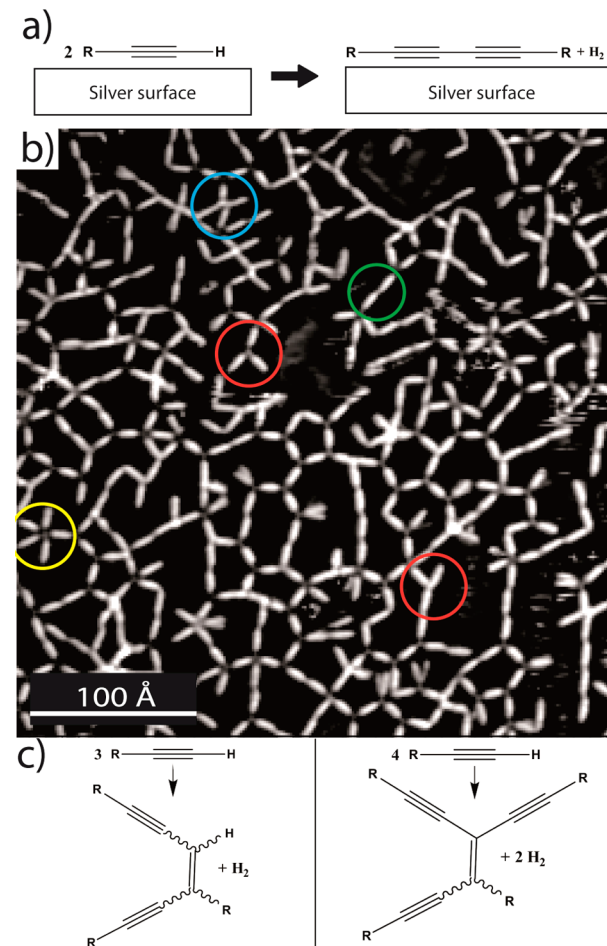


Figure 1. (a) Schematic representation of the targeted linear covalent homocoupling reaction of the terminal acetylenic compounds with the Ag(111) surface as a catalyst. (b) STM image ($U_{Bias} = -290$ mV, $I_t = 0.075$ nA) of a polymerized, irregular porous network fabricated by annealing **1** on the Ag(111) substrate to 400 K. Reaction products resulting from covalent coupling of two, three, four, or even five monomers are highlighted in green, red, blue, and yellow, respectively. Strict chemoselectivity as required for the targeted, linear reaction depicted in (a) is impeded by the various side reactions as cis/trans hydrogenations and multiple insertion reactions. (c) Examples of side reactions involving three and four reacting monomers.

circle) are formed, they represent a minority product (34.2% yield). The dominating branched products, where three (46.8%, red) or four (15.2%, blue) end groups merge, reflect further reactions associated with cis/trans hydrogenations, multiple insertion reactions, and/or possibly cyclotrimerization that markedly reduce the chemoselectivity. More complex structures obtained from five monomers (3.8%, yellow circle) can be attributed to the cross-insertion involving monomers and its dimers at once. Considering the encountered wide variety of different mechanisms for polymerization reactions, the simple use of planar surfaces is obviously not ideal to fabricate either hydrocarbon molecular wires or 2D periodic lattices via acetylenic coupling.

Inspired by the templating concepts developed in solution chemistry^{10–12} and recent related developments using metal-directed assembly at surfaces to direct covalent reactions,⁵⁵ we thus devised an improved synthesis protocol, utilizing a vicinal surface. The special properties of the provided step edges have been employed in the past regarding their increased catalytic activity^{56,57} or to steer the assembly of 1D supramolecular wires⁵⁸ or nanoribbons.⁵⁹ To direct the C–C coupling reaction toward the formation of linear butadiyne scaffolds, we used the Ag(877) vicinal surface, which can be expressed in the high index Miller notation as (S) – [15(111) × (100)]. Ideally, this template consists of regularly alternating terraces (15 atomic rows along the [112] direction) and (100)-microfacets. The theoretical values for terrace width and step height are $W = 36.6 \text{ \AA}$ and $h = 2.35 \text{ \AA}$, respectively. The real Ag(877) surface exhibits a distribution of terrace widths around the ideal value separated by monatomic steps (cf. Figure 2b–d).

To identify the favorable adsorption sites of **1**, a small concentration of molecules was evaporated onto the Ag(877) template held at 186 K. Figure 2b reveals that the molecules, appearing as bright rods, bind to the lower step edges with their backbone parallel to the latter, as can be seen in the superimposed model in the inset. This step decoration persists at increased coverage (Figure 2c).

Importantly, as the molecule–substrate interaction prevails, not a single molecular unit deviates from the preferred alignment. This demonstrates that with vicinal surfaces the monomer alignment can be steered with atomic precision, creating a prospective arrangement for subsequent polymerization. The templating effect is ascribed to noncovalent interactions between the rodlike molecules and the step-edge atoms,⁶⁰ although the terminal ethyne groups repel each other in linear arrangements due to the polarity of the C–H bond.⁶¹ Thus, at low concentrations agglomeration via the known T-shaped or other ordering motifs of alkyne groups are inhibited.^{61–63} A related equidistant lateral spacing mediated by indirect interaction was reported for other organic units at low-index metal surfaces.^{64–68}

In order to trigger the formation of covalent bonds between the terminal ethyne groups, we annealed a sample with the ideal prereaction ordering (similar to Figure 2c) to 450 K. The result is displayed in Figure 2d, where extended and connected structures along the step edges are discernible. These chain features are clearly distinct from the low-temperature arrangements and exhibit a continuous structure presenting a succession of spheroidal units.

To prove that the formed bonds between the monomers are consistent with the covalent homocoupling identified at the flat Ag(111) surface, we performed several tests. First, we measured the distance d between neighboring molecules in the low-

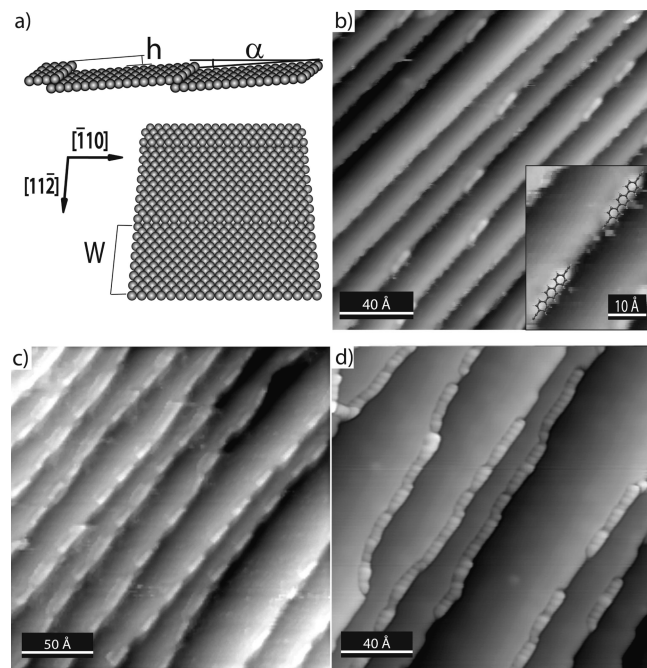


Figure 2. (a) Model of the ideal Ag(877) surface with a terrace width of $W = 36.6 \text{ \AA}$, step height $h = 2.35 \text{ \AA}$ and miscut angle $\alpha = 3.67^\circ$ with respect to the (111) plane. (b) STM image showing the preferential step-edge decoration upon exposure to small amounts of **1**; inset highlights two monomers with their models superimposed ($U_{\text{Bias}} = -1.0 \text{ V}$, $I_t = 0.06 \text{ nA}$). (c) Regular alignment close to step-edge saturation at low temperature ($U_{\text{Bias}} = -1.03 \text{ V}$, $I_t = 0.08 \text{ nA}$). (d) After annealing the sample to 450 K extended connected structures are present at the (100) microfacets with submolecular features resolved ($U_{\text{Bias}} = -1.08 \text{ V}$, $I_t = 0.07 \text{ nA}$). To emphasize step-edge features, the data are presented by subtracting an average plane of the entire image leading to a variable contrast of the terraces related to their widths.

temperature phase before annealing, as shown in Figure 3a. The pertaining line profile reveals that molecules adsorb equidistantly with a periodicity of $d = 22.9 \pm 1.8 \text{ \AA}$. This value varies appreciably as the 1D molecular density at the step depends sensitively on the surface coverage. Measuring the related periodicity d^* (Figure 3b) following annealing (cf. Figure 2d) gives a value of $d^* = 17.9 \pm 0.6 \text{ \AA}$, which is significantly smaller than the d in the self-assembled 1D phase and smaller than the length of a single molecule (cf. Scheme 1). The theoretical value 8.56 \AA between the two benzene rings at both ends of **1** can be nicely compared with the experimental value $l_{b1-b3} = 8.4 \pm 0.6 \text{ \AA}$ (Figure 3b), indicating an intact structure of the molecular backbone. Considering these findings, the corrugation in the line profile is associated with the three arene rings of **1**, connected by newly formed butadiyne bridges, which corresponds to a terphenylene-butadiynylene compound. Note that some of the formed bonds show a protrusion instead of a depression, as indicated with an arrow in Figure 3b, even though the distance d^* remains constant. The invariance in d^* would in principle refute the idea of a possible Ag-bisacetylide compound (cf. discussion in ref 36), indicating the presence of an impurity.

To further corroborate the C–C coupling between terminal alkynes and the intactness of the molecular backbone, a high-resolution image of a three units section of a coupled molecular wire is analyzed (Figure 3c). The direct real-space visualization reveals a clear distinguishability between the benzene rings, which appear as bright protrusions in groups of three, and the

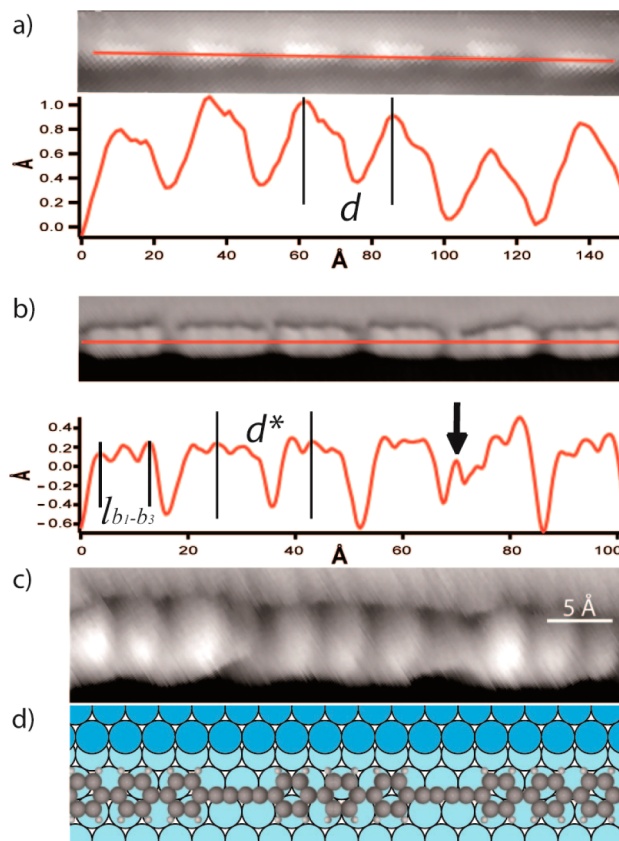


Figure 3. (a) STM image of six-membered molecular segment at a step edge in the low-temperature phase. The line profile (red) shows an intermolecular distance of $d = 22.9 \pm 1.8 \text{ \AA}$ ($U_{\text{Bias}} = -1.03 \text{ V}$, $I_t = 0.08 \text{ nA}$). (b) STM image of six polymerized molecules ($U_{\text{Bias}} = -0.5 \text{ V}$, $I_t = 0.12 \text{ nA}$). The distances between the center of two adjacent monomers and the external peaks in every trio are defined as d^* and l_{b1-b3} . The experimental line profile (red line) gives the values $d^* = 17.9 \pm 0.6 \text{ \AA}$ and $l_{b1-b3} = 8.4 \pm 0.6 \text{ \AA}$. (c) High-resolution STM image of a part of a terphenylene-butadiynylene wire placed at the lower step-edge ($U_{\text{Bias}} = -1.5 \text{ V}$, $I_t = 0.05 \text{ nA}$). (d) Model of the situation depicted in c with the chemical structure of the wire and the registry with the underlying Ag(877) substrate. Dark blue and light blue refer to the upper and lower terrace edge, respectively. Panels c and d are of the same scale.

newly formed covalent linkages appearing as depressions. This image is part of a series of consecutive topographs where surface atoms were resolved aside the molecules (see Supporting Information Figure S2). Accordingly, we can obtain precise measures of the adsorption geometry. Figure 3d presents a model for a segment of an ideal terphenylene-butadiynylene wire on the Ag(877) template. For comparison the geometry of an isolated and infinitely long polymer was geometrically optimized within the DFT framework assuming periodic boundary conditions. Both the positioning of the submolecular features and the theoretical periodicity of $d_t^* = 18.21 \text{ \AA}$ agree well with the experimental data, giving additional evidence that the formed bridges consist of butadiyne moieties. The registry of the wire in the model is obtained by superimposing the calculated wire on the STM data (Supporting Information Figure S2) and incommensurability along the [110] direction is found, which is in line with the specific C–C bond length in a covalent architecture. We also compared the agreement of the experimental data with an alternative explanation of the covalent linkage. The investigated

different final product in which one triple bond is replaced by a double bond could not explain the topographic contrast in a satisfying way (see Supporting Information Figure S3), confirming that the model proposed in Figure 3c describes the real nature.

By employing 1D templating on vicinal surface, the chemoselectivity of the targeted linear homocoupling can thus be increased to become the dominant reaction with a massively increased yield (determined to be 85.4% when starting with regular step-decoration, see Supporting Information Figure S4). Although it was not possible to monitor the homocoupling reaction *in situ*, it is suggested that the templating effect persists at higher temperatures resulting in a preferred 1D molecular diffusion along the step edge mediating the thermally activated covalent bond formation. By favoring the parallel alignment of the molecular backbone with respect to the step orientation, a linear arrangement of the reaction product and hence a chemoselective pathway is predetermined. Taking into account that the vicinal surface provides step edge arrays on the macroscopic scale, our method establishes the production of highly anisotropic novel hydrocarbon material with atomic precision.

Finally, to test the stability of the fabricated molecular wires, *in situ* chain manipulations by laterally displacing the STM tip in the constant current mode were carried out (Figure 4).^{69,70}

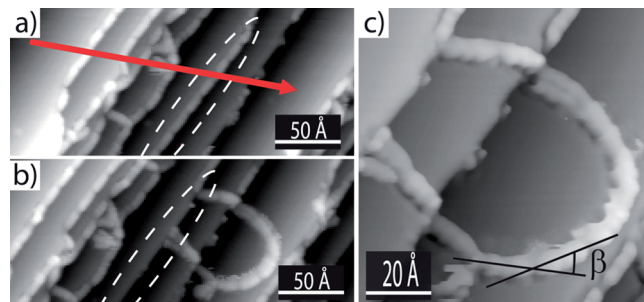


Figure 4. (a) Direct manipulation of a terphenylene-butadiynylene chain chain. ($U_{\text{Bias}} = -0.98 \text{ V}$, $I_t = 0.1 \text{ nA}$). The red arrow indicates the path of the tip manipulation and the white dashed ellipse highlights the segment to be displaced. (b) Same area after performing the lateral manipulation (Parameters: $U_{\text{bias}} = 0.1 \text{ V}$, $I_t = 20 \text{ nA}$) using constant-current mode imaging ($U_{\text{Bias}} = -0.98 \text{ V}$, $I_t = 0.1 \text{ nA}$). (c) Zoomed-in image of the detached segment of 1 polymer ($U_{\text{Bias}} = -0.5 \text{ V}$, $I_t = 0.1 \text{ nA}$). Butadiyne bridges exhibit a significant flexibility with an angle β between neighboring monomers in the range of 25° to 40° .

By employing this method, molecular wires can be even detached from the step edge to be further analyzed. The path of the tip is depicted by a red arrow in Figure 4a, and the result of the lateral manipulation is shown in Figure 4b. In this process, a segment of a polymer wire is strongly distorted, while keeping its topologic integrity. Further manipulations (see Supporting Information Figure S5) show that this segment can be displaced from across the terraces, without breaking any of the formed covalent bonds. This is a further proof of the robust linkages between the building blocks and corroborates the potential for transfer to other substrates. The butadiyne groups demonstrate an impressive flexibility, as can be appreciated in Figure 4c, in which the 11 molecules can be distinguished from each other, forming an almost closed circle. On the lower terrace, the angles enclosed by the long axes of two neighboring

units (Figure 4c) cover a range from 25° to 40° with an average value of $\beta = 32 \pm 7^\circ$.

Our method demonstrates the chemoselective synthesis of linear polymers of high purity. In contrast to the so far reported graphdiyne wires,^{71–73} we introduced a scaffold with alternating para-ter-phenylene and butadiyne instead of phenylene and ethynyl, therefore we refer to it as extended graphdiyne wire. One example in which 15 monomers have been coupled to a polymer with a length of 270 \AA is depicted in Figure 5a. Thus,

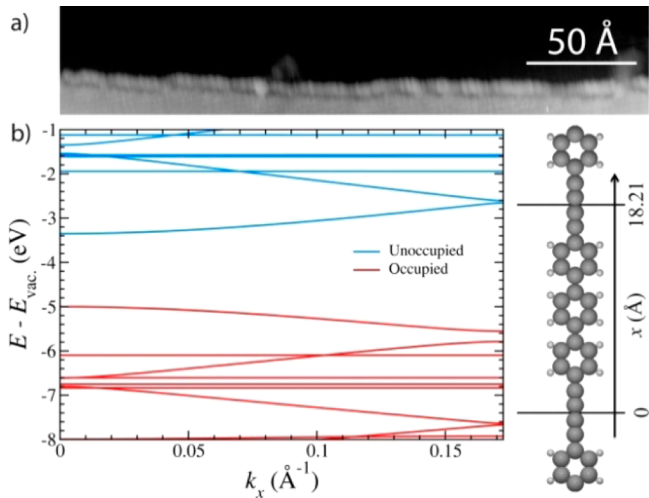


Figure 5. (a) STM image of a ca. 268 \AA long polymer, by successfully covalently linking at least 15 monomers ($U_{\text{Bias}} = -1.08 \text{ V}$, $I_t = 0.07 \text{ nA}$). (b) Electronic band structure (left) obtained from DFT calculations of an infinite 1D polymer (right) as a function of the wave vector k_x .

the length of the molecular wire amounts to more than two times the lengths of the longest reported phenylene-ethynylene oligomer¹⁵ or oligo(p-phenylene-butadiynylene) rod.⁴⁶ For an investigation of the electronic properties of the 1D material, we performed DFT calculations as described in more detail in the Supporting Information, computing the electronic band structure of an infinite defect-free 1D wire without any interaction with the substrate. The band structure as a function of the wave vector k_x is displayed in Figure 5b, where red and blue lines correspond to occupied and unoccupied states, respectively. The energy gap between the highest occupied electronic band and the lowest unoccupied one is ca. 1.6 eV . It has to be taken into account that DFT severely underestimates band gaps. Furthermore, the band structure, which was calculated assuming coplanar alignment of all phenylene units, depends on their relative orientations. For the energy-optimized twisted geometry (see Supporting Information Figure S6) the energy gap is increased and the band dispersions are smaller, which is in agreement with general tendencies for similar molecular wires,^{74,75} however no qualitative changes are induced by the twisting. The presence of the surface is expected to counteract such potential gap augmentations. Prior results⁵⁹ suggest that the energy gap decreases when the species is sitting on a metal surface, as an effect of the surface polarization. Independent from these effects, the maxima of the occupied states and the minima of the unoccupied are both at $k_x = 0$, therefore the ideal terphenylene-butadiynylene wire constitutes a direct band gap organic semiconductor.

At this stage it is worth noting that the highest valence and the lowest conduction band exhibit a nearly cosine shape and in contrast to graphyne and graphdiyne nanoribbons^{71,73} are free from band crossings. These are ideal qualifications for the manifestation of intriguing nonlinear electronic transport physics related to Bloch oscillations.^{76,77} With similarly shaped bands in semiconductor superlattices, high-frequency devices like gigahertz generators^{78,79} and terahertz detectors⁸⁰ have been realized. With the very different conditions present in the novel 1D material we expect exciting new possibilities for such applications.

In conclusion, we have demonstrated a novel method to select a specific reaction from a set of several entangled ones in a surface-assisted molecular engineering scenario. By confining the terminal alkyne reactants to step edges of a vicinal Ag(877) template, chemoselective butadiyne formation is preferred over branching side-reactions encountered on the planar silver surface. We use this approach for the atomically precise fabrication of a novel conjugated molecular wire that is part of the family of extended graphdienes. A first assessment of its electronic properties qualifies the new material as a 1D semiconductor with a prosperously simple band structure with the desirable small energy gap. Furthermore, the stepped surface accomplishes at the same time a parallel alignment of the wires, affording the creation of macroscopically highly anisotropic materials. With this method, an entire set of novel carbon scaffolds comes in reach. Moreover, it is not limited to the synthesis of carbon-rich materials but should be transferable to a large variety of buildings blocks and reactions. In this regard, we contributed to the advancement of covalent bottom-up nanofabrication strategies in which the exquisite control of the atomic environment for complex reaction pathways is decisive to unfold their full potential.

■ ASSOCIATED CONTENT

§ Supporting Information

Detailed information about the synthesis of the novel compound 4,4"-diethynyl-1,1':4'1"terphenyl. STM image simultaneously resolving the novel compound and the surface atoms to deduce the adsorption geometry. Comparison between two a priori compatible descriptions of the molecular chain, which differentiates the reaction scheme. Exemplary data showing the ratio of chemoselectivity of the linear homocoupling achieved by templating the reaction on the Ag(877). The sequence of manipulations on the same displaced segment highlights the versatility of the formed wire. Details on the DFT calculation of the band structure of the ideal polymer. This material is available free of charge via the Internet at <http://pubs.acs.org>.

■ AUTHOR INFORMATION

Corresponding Author

*E-mail: florian.klappenberger@tum.de.

Author Contributions

The manuscript was written through contributions of all authors. All authors have given approval to the final version of the manuscript.

Notes

The authors declare no competing financial interest.

ACKNOWLEDGMENTS

M.R. would like to thank for the generous support by the DFG-priority program 1459. Work supported by the European Union via ERC Advanced Grant MolArt (no. 247299) and Chinese Scholarship Council.

REFERENCES

- (1) Diederich, F.; Rubin, Y. *Angew. Chem., Int. Ed.* **1992**, *31* (9), 1101–1123.
- (2) Diederich, F. *Nature* **1994**, *369* (6477), 199–207.
- (3) Bunz, U. H. F.; Rubin, Y.; Tobe, Y. *Chem. Soc. Rev.* **1999**, *28* (2), 107–119.
- (4) Hirsch, A. *Nat. Mater.* **2010**, *9* (11), 868–871.
- (5) Diederich, F.; Kivala, M. *Adv. Mater.* **2010**, *22* (7), 803–812.
- (6) Enyashin, A. N.; Ivanovskii, A. L. *Phys. Status Solidi B* **2011**, *248* (8), 1879–1883.
- (7) Ivanovskii, A. L. *Prog. Solid State Chem.* **2013**, *41* (1–2), 1–19.
- (8) Siemsen, P.; Livingston, R. C.; Diederich, F. *Angew. Chem., Int. Ed.* **2000**, *39* (15), 2632–2657.
- (9) Diederich, F. *Chem. Commun.* **2001**, *03*, 219–227.
- (10) Anderson, S.; Anderson, H. L.; Sanders, J. K. M. *Acc. Chem. Res.* **1993**, *26* (9), 469–475.
- (11) Fang, L.; Basu, S.; Sue, C. H.; Fahrenbach, A. C.; Stoddart, J. F. *J. Am. Chem. Soc.* **2011**, *133* (3), 396–399.
- (12) O’Sullivan, M. C.; Sprafke, J. K.; Kondratuk, D. V.; Rinfray, C.; Claridge, T. D. W.; Saywell, A.; Blunt, M. O.; O’Shea, J. N.; Beton, P. H.; Malfois, M.; Anderson, H. L. *Nature* **2011**, *469* (7328), 72–75.
- (13) Bunz, U. H. F. *Macromol. Rapid Commun.* **2009**, *30* (9–10), 772–805.
- (14) Jones, L.; Schumm, J. S.; Tour, J. M. *J. Org. Chem.* **1997**, *62* (5), 1388–1410.
- (15) Schumm, J. S.; Pearson, D. L.; Tour, J. M. *Angew. Chem., Int. Ed. Engl.* **1994**, *33* (13), 1360–1363.
- (16) Grimsdale, A. C.; Chan, K. L.; Martin, R. E.; Jokisz, P. G.; Holmes, A. B. *Chem. Rev.* **2009**, *109* (3), 897–1091.
- (17) Facchetti, A. *Chem. Mater.* **2011**, *23* (3), 733–758.
- (18) Kulkarni, A. P.; Tonzola, C. J.; Babel, A.; Jenekhe, S. A. *Chem. Mater.* **2004**, *16* (23), 4556–4573.
- (19) Jiang, J. X.; Su, F.; Niu, H.; Wood, C. D.; Campbell, N. L.; Khimyak, Y. Z.; Cooper, A. I. *Chem. Commun.* **2008**, *4*, 486–488.
- (20) Martin, R. E.; Diederich, F. *Angew. Chem., Int. Ed.* **1999**, *38* (10), 1350–1377.
- (21) Tour, J. M. *Chem. Rev.* **1996**, *96* (1), 537–553.
- (22) Bae, S.; Kim, H.; Lee, Y.; Xu, X. F.; Park, J. S.; Zheng, Y.; Balakrishnan, J.; Lei, T.; Kim, H. R.; Song, Y. I.; Kim, Y. J.; Kim, K. S.; Ozilmez, B.; Ahn, J. H.; Hong, B. H.; Iijima, S. *Nat. Nanotechnol.* **2010**, *5* (8), 574–578.
- (23) Grill, L.; Dyer, M.; Lafferentz, L.; Persson, M.; Peters, M. V.; Hecht, S. *Nat. Nanotechnol.* **2007**, *2* (11), 687–691.
- (24) Lafferentz, L.; Ample, F.; Yu, H.; Hecht, S.; Joachim, C.; Grill, L. *Science* **2009**, *323* (5918), 1193–1197.
- (25) Cai, J. M.; Ruffieux, P.; Jaafar, R.; Bieri, M.; Braun, T.; Blankenburg, S.; Muoth, M.; Seitsonen, A. P.; Saleh, M.; Feng, X. L.; Müllen, K.; Fasel, R. *Nature* **2010**, *466* (7305), 470–473.
- (26) Wang, W.; Shi, X.; Wang, S.; Van Hove, M. A.; Lin, N. *J. Am. Chem. Soc.* **2011**, *133* (34), 13264–13267.
- (27) Fan, Q.; Wang, C.; Han, Y.; Zhu, J.; Hieringer, W.; Kuttner, J.; Hilt, G.; Gottfried, J. M. *Angew. Chem., Int. Ed.* **2013**, *52* (17), 4668–4672.
- (28) Schmitz, C. H.; Ikonomov, J.; Sokolowski, M. *J. Phys. Chem. C* **2009**, *113* (28), 11984–11987.
- (29) Schmitz, C. H.; Schmid, M.; Gärtnert, S.; Steinrück, H.-P.; Gottfried, J. M.; Sokolowski, M. *J. Phys. Chem. C* **2011**, *115* (37), 18186–18194.
- (30) Schmitz, C. H.; Ikonomov, J.; Sokolowski, M. *J. Phys. Chem. C* **2011**, *115* (15), 7270–7278.
- (31) Matena, M.; Riehm, T.; Stöhr, M.; Jung, T. A.; Gade, L. H. *Angew. Chem., Int. Ed.* **2008**, *47* (13), 2414–2417.
- (32) Matena, M.; Stöhr, M.; Riehm, T.; Björk, J.; Martens, S.; Dyer, M. S.; Persson, M.; Lobo-Checa, J.; Müller, K.; Enache, M.; Wadeholt, H.; Zegenhagen, J.; Jung, T. A.; Gade, L. H. *Chem.—Eur. J.* **2010**, *16* (7), 2079–2091.
- (33) Weigelt, S.; Busse, C.; Bombis, C.; Knudsen, M. M.; Gothelf, K. V.; Strunkus, T.; Wöll, C.; Dahlbom, M.; Hammer, B.; Lægsgaard, E.; Besenbacher, F.; Linderoth, T. R. *Angew. Chem., Int. Ed.* **2007**, *46* (48), 9227–9230.
- (34) Abel, M.; Clair, S.; Ourdjini, O.; Mossoyan, M.; Porte, L. *J. Am. Chem. Soc.* **2011**, *133* (5), 1203–1205.
- (35) Dienstmaier, J. F.; Medina, D. D.; Dogru, M.; Knochel, P.; Bein, T.; Heckl, W. M.; Lackinger, M. *ACS Nano* **2012**, *6* (8), 7234–7242.
- (36) Zhang, Y.-Q.; Kepčija, N.; Kleinschrodt, M.; Diller, K.; Fischer, S.; Papageorgiou, A. C.; Allegretti, F.; Björk, J.; Klyatskaya, S.; Klappenberg, F.; Ruben, M.; Barth, J. V. *Nat. Commun.* **2012**, *3*, 1286–1–8.
- (37) Björk, J.; Zhang, Y.-Q.; Klappenberg, F.; Barth, J. V.; Stafström, S. *J. Phys. Chem. C* **2014**, *118* (6), 3181–3187.
- (38) Eichhorn, J.; Heckl, W. M.; Lackinger, M. *Chem. Commun.* **2013**, *49* (28), 2900–2902.
- (39) Gao, H. Y.; Wagner, H.; Zhong, D. Y.; Franke, J. H.; Studer, A.; Fuchs, H. *Angew. Chem., Int. Ed.* **2013**, *52* (14), 4024–4028.
- (40) Cirera, B.; Zhang, Y.-Q.; Klyatskaya, S.; Ruben, M.; Klappenberg, F.; Barth, J. V. *ChemCatChem* **2013**, *5* (11), 3281–3288.
- (41) Gao, H.-Y.; Franke, J.-H.; Wagner, H.; Zhong, D.; Held, P.-A.; Studer, A.; Fuchs, H. *J. Phys. Chem. C* **2013**, *117* (36), 18595–18602.
- (42) Arado, O. D.; Möning, H.; Wagner, H.; Franke, J. H.; Langewisch, G.; Held, P. A.; Studer, A.; Fuchs, H. *ACS Nano* **2013**, *7* (10), 8509–8515.
- (43) Bebensee, F.; Bombis, C.; Vadapoo, S. R.; Cramer, J. R.; Besenbacher, F.; Gothelf, K. V.; Linderoth, T. R. *J. Am. Chem. Soc.* **2013**, *135* (6), 2136–2139.
- (44) Zhong, D.; Franke, J.-H.; Podiyannachari, S. K.; Blömkér, T.; Zhang, H.; Kehr, G.; Erker, G.; Fuchs, H.; Chi, L. *Science* **2011**, *334* (6053), 213–216.
- (45) Cooper, A. I. *Adv. Mater.* **2009**, *21* (12), 1291–1295.
- (46) Mössinger, D.; Jester, S. S.; Sigmund, E.; Müller, U.; Höger, S. *Macromolecules* **2009**, *42* (20), 7974–7978.
- (47) Ambrosch-Draxl, C.; Puschnig, P.; Resel, R.; Leising, G. *Synth. Met.* **1999**, *101* (1–3), 673–674.
- (48) Puschnig, P.; Ambrosch-Draxl, C. *Phys. Rev. B* **1999**, *60* (11), 7891–7898.
- (49) Koller, G.; Berkebile, S.; Oehzelt, M.; Puschnig, P.; Ambrosch-Draxl, C.; Netzer, F. P.; Ramsey, M. G. *Science* **2007**, *317* (5836), 351–355.
- (50) Kresse, G.; Furthmüller, J. *Phys. Rev. B* **1996**, *54* (16), 11169–11186.
- (51) Blöchl, P. E. *Phys. Rev. B* **1994**, *50* (24), 17953–17979.
- (52) Perdew, J. P.; Burke, K.; Ernzerhof, M. *Phys. Rev. Lett.* **1996**, *77* (18), 3865–3868.
- (53) Klyatskaya, S.; Klappenberg, F.; Schlickum, U.; Kühne, D.; Marschall, M.; Reichert, J.; Decker, R.; Krenner, W.; Zoppellaro, G.; Brune, H.; Barth, J. V.; Ruben, M. *Adv. Funct. Mater.* **2011**, *21* (7), 1230–1240.
- (54) Patwari, G. N.; Venugopalan, P.; Kolaski, M. *Chem. Phys.* **2013**, *415*, 150–155.
- (55) Lin, T.; Shang, X. S.; Adisojoso, J.; Liu, P. N.; Lin, N. *J. Am. Chem. Soc.* **2013**, *135* (9), 3576–3582.
- (56) Zambelli, T.; Wintterlin, J.; Trost, J.; Ertl, G. *Science* **1996**, *273* (5282), 1688–1690.
- (57) Saywell, A.; Schwarz, J.; Hecht, S.; Grill, L. *Angew. Chem., Int. Ed.* **2012**, *51* (21), 5096–5100.
- (58) Cañas-Ventura, M. E.; Xiao, W.; Wasserfallen, D.; Müllen, K.; Brune, H.; Barth, J. V.; Fasel, R. *Angew. Chem., Int. Ed.* **2007**, *46* (11), 1814–1818.
- (59) Ruffieux, P.; Cai, J. M.; Plumb, N. C.; Patthey, L.; Prezzi, D.; Ferretti, A.; Molinari, E.; Feng, X. L.; Müllen, K.; Pignedoli, C. A.; Fasel, R. *ACS Nano* **2012**, *6* (8), 6930–6935.

- (60) Vladimirova, M.; Stengel, M.; De Vita, A.; Baldereschi, A.; Böhringer, M.; Morgenstern, K.; Berndt, R.; Schneider, W. D. *Europhys. Lett.* **2001**, *56* (2), 254–260.
- (61) Philp, D.; Robinson, J. M. A. *J. Chem. Soc., Perkin Trans. 2* **1998**, No. (7), 1643–1650.
- (62) Kepčija, N.; Zhang, Y.-Q.; Kleinschrodt, M.; Björk, J.; Klyatskaya, S.; Klappenberger, F.; Ruben, M.; Barth, J. V. *J. Phys. Chem. C* **2013**, *117* (39), 3987–3995.
- (63) Li, Q.; Han, C.; Horton, S. R.; Fuentes-Cabrera, M.; Sumpter, B. G.; Lu, W.; Bernholc, J.; Maksymovych, P.; Pan, M. *ACS Nano* **2011**, *6* (1), 566–572.
- (64) Bischoff, F.; Seufert, K.; Auwärter, W.; Joshi, S.; Vijayaraghavan, S.; Ecija, D.; Diller, K.; Papageorgiou, A. C.; Fischer, S.; Allegretti, F.; Duncan, D. A.; Klappenberger, F.; Blobner, F.; Han, R. Y.; Barth, J. V. *ACS Nano* **2013**, *7* (4), 3139–3149.
- (65) Tomba, G.; Stengel, M.; Schneider, W. D.; Baldereschi, A.; De Vita, A. *ACS Nano* **2010**, *4* (12), 7545–7551.
- (66) Wagner, C.; Kasemann, D.; Golnik, C.; Forker, R.; Esslinger, M.; Müllen, K.; Fritz, T. *Phys. Rev. B* **2010**, *81* (3), 035423–1–6.
- (67) Diller, K.; Klappenberger, F.; Allegretti, F.; Papageorgiou, A. C.; Fischer, S.; Wiengarten, A.; Joshi, S.; Seufert, K.; Ecija, D.; Auwärter, W.; Barth, J. V. *J. Chem. Phys.* **2013**, *138* (15), 154710–1–9.
- (68) Fernandez-Torrente, I.; Monturet, S.; Franke, K. J.; Fraxedas, J.; Lorente, N.; Pascual, J. *I. Phys. Rev. Lett.* **2007**, *99* (17), 176103–1–4.
- (69) Heim, D.; Ecija, D.; Seufert, K.; Auwärter, W.; Aurisicchio, C.; Fabbro, C.; Bonifazi, D.; Barth, J. V. *J. Am. Chem. Soc.* **2010**, *132* (19), 6783–6790.
- (70) Marschall, M.; Reichert, J.; Weber-Bargioni, A.; Seufert, K.; Auwärter, W.; Klyatskaya, S.; Zoppellaro, G.; Ruben, M.; Barth, J. V. *Nature Chem.* **2010**, *2* (2), 131–137.
- (71) Bai, H. C.; Zhu, Y.; Qiao, W. Y.; Huang, Y. H. *RSC Adv.* **2011**, *1* (5), 768–775.
- (72) Qian, X. M.; Ning, Z. Y.; Li, Y. L.; Liu, H. B.; Ouyang, C. B.; Chen, Q.; Li, Y. *J. Dalton Trans.* **2012**, *41* (3), 730–733.
- (73) Pan, L. D.; Zhang, L. Z.; Song, B. Q.; Du, S. X.; Gao, H. *J. Appl. Phys. Lett.* **2011**, *98* (17), 173102–1–3.
- (74) Brocorens, P.; Zojer, E.; Cornil, J.; Shuai, Z.; Leising, G.; Müllen, K.; Bredas, J. L. *Synth. Met.* **1999**, *100* (1), 141–162.
- (75) Tomfohr, J.; Sankey, O. F. *J. Chem. Phys.* **2004**, *120* (3), 1542–1554.
- (76) Bloch, F. *Z. Phys.* **1928**, *52*, 555–600.
- (77) Ignatov, A. A.; Renk, K. F.; Dodin, E. P. *Phys. Rev. Lett.* **1993**, *70* (13), 1996–1999.
- (78) Klappenberger, F.; Renk, K. F.; Renk, P.; Rieder, B.; Koshurinov, Y. I.; Pavlev, D. G.; Ustinov, V.; Zhukov, A.; Maleev, N.; Vasilyev, A. *Appl. Phys. Lett.* **2004**, *84* (19), 3924–3926.
- (79) Waschke, C.; Roskos, H. G.; Schwedler, R.; Leo, K.; Kurz, H.; Köhler, K. *Phys. Rev. Lett.* **1993**, *70* (21), 3319–3322.
- (80) Klappenberger, F.; Ignatov, A. A.; Winnerl, S.; Schomburg, E.; Wegscheider, W.; Renk, K. F.; Bichler, M. *Appl. Phys. Lett.* **2001**, *78* (12), 1673–1675.